Pergamon

Chaos, Solitons & Fractals Vol. 10, No. 4–5, pp. 701–707, 1999
© 1999 Elsevier Science Ltd. All rights reserved
0960–0779/99/$ - see front matter

PII: S0960-0779(98)00018-6

Origin and Control of Dynamics of Hexagonal Patterns in a Photorefractive Feedback System

M. SCHWAB,† M. SEDLATSCHEK, B. THÜRING, C. DENZ and T. TSCHUDI

Institut für Angewandte Physik, Technische Universität Darmstadt, Hochschulstr. 6, D-64289 Darmstadt, Germany

Abstract—We investigate the origin of dynamics of hexagonal pattern formation in a photorefractive single feedback system. By introducing an asymmetry, we induced different complex motion behaviours. A visualization method is presented and means to control the dynamics in the case of fixed external parameters are discussed. © 1999 Elsevier Science Ltd. All rights reserved.

1. TRANSVERSE STRUCTURES IN PHOTOREFRACTIVE MEDIA

In a variety of nonlinear optical media, spontaneous pattern formation due to light beam interaction can be observed. For collinear pump beams, the cylindrical symmetry of the configuration around the propagation axis gives rise to a predominantly hexagonal structure. Previous experiments were performed using atomic vapor [1], liquid crystals [2], liquid crystal light valves [3], bacteriorhodopsin[4] and photorefractive crystals [5, 6].

A linear stability analysis of the coupled differential equations for the case of contradirectional two-wave mixing was performed recently [7]. Above a certain threshold, the light intensity profile shows a modulational instability in the transverse direction, giving rise to spatial sidebands with a certain transverse wave vector K_T, determined by the minimum of the corresponding threshold curve. A self-organizing process then leads to an equidistant spot array in the far field determined by the same K_T. The simplest realization of this condition is a complete hexagonal structure which can be monitored in the far field or as a honeycomb structure in the near field [see Fig. 1(a,b)]. Here, we present investigations on the origin and control of hexagonal pattern dynamics arising in a photorefractive single feedback system. After recalling the theoretical aspects, we introduce the experimental setup and the essential properties of this system. A method to visualize the dynamics of hexagonal pattern is presented and different motion behaviours are discussed.

2. THEORETICAL TREATMENT

A schematic representation of the studied system is given in Fig. 2. The photorefractive medium is pumped by a frequency-doubled Nd:YAG Laser ($\lambda = 532\,\text{nm}$). Using a thin biconvex lens, a double-pass $2f$–$2f$ imaging system with a feedback mirror at its end provides the feedback beam.

† Author for correspondence. E-mail: michael.schwab@physik.tu-darmstadt.de.

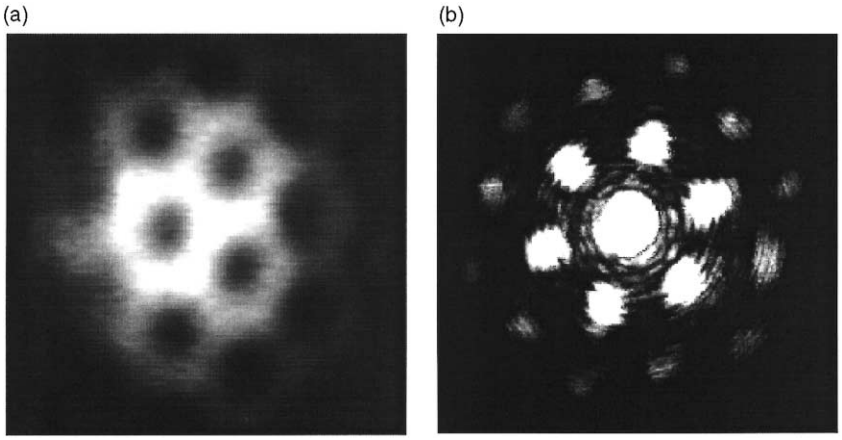

Fig. 1. (a) Honeycomb structure in the near field (image of the beam at the end of the crystal). (b) Hexagonal structure in the far field with second and third harmonics.

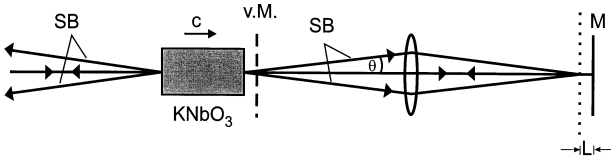

Fig. 2. Schematic experimental setup—SB = spatial sidebands, M = mirror, v.M. = virtual mirror, L = propagation length.

Using ABCD matrices, one can show that this system is not completely equivalent to a simple mirror feedback setup, but it has the advantage that the virtual mirror can be moved even inside the crystal by moving the feedback mirror, i.e., negative propagation lengths can be achieved. The physical role of the feedback path with a virtual mirror position L from the crystal is to introduce a phase lag of $k_0\theta^2 L$ between the pump (or the feedback) and the emerging sidebands emitted at an angle θ with respect to the propagation axis.

To analyze the threshold condition for the instability of wave vectors in the transverse plane, we start with the usual two-wave mixing equations, taking into account the beam profile in the transverse direction. With the assumption that reflection gratings are dominant in this configuration, these coupling equations can be written as [7]

$$\frac{\partial F}{\partial z} - \frac{i}{2k_0 n_0}\nabla_\perp^2 F = i\gamma \frac{|B|^2}{|F|^2 + |B|^2} F \tag{1}$$

$$\frac{\partial B}{\partial z} + \frac{i}{2k_0 n_0}\nabla_\perp^2 B = -i\gamma^* \frac{|F|^2}{|F|^2 + |B|^2} B \tag{2}$$

where F and B are the amplitudes of the forward and backward wave (pump and feedback), z is the direction of propagation, k_0 the wave number in vacuum, n_0 denotes the linear refractive index of the nonlinear medium, γ is the complex photorefractive coupling coefficient and $\nabla_\perp^2$ denotes the transverse Laplacian. The amplitudes of the forward and backward wave with weak modulations of wave vector $\vec{k}_\perp$ in the transverse direction can be written as

$$F(\vec{r}) = F_0(z) \times [1 + F_{+1}(z)\exp(i\vec{k}_\perp \cdot \vec{r}_\perp) + F_{-1}(z)\exp(-i\vec{k}_\perp \cdot \vec{r}_\perp)] \tag{3}$$

$$B(\vec{r}) = B_0(z) \times [1 + B_{+1}(z)\exp(i\vec{k}_\perp \cdot \vec{r}_\perp) + B_{-1}(z)\exp(-i\vec{k}_\perp \cdot \vec{r}_\perp)] \tag{4}$$

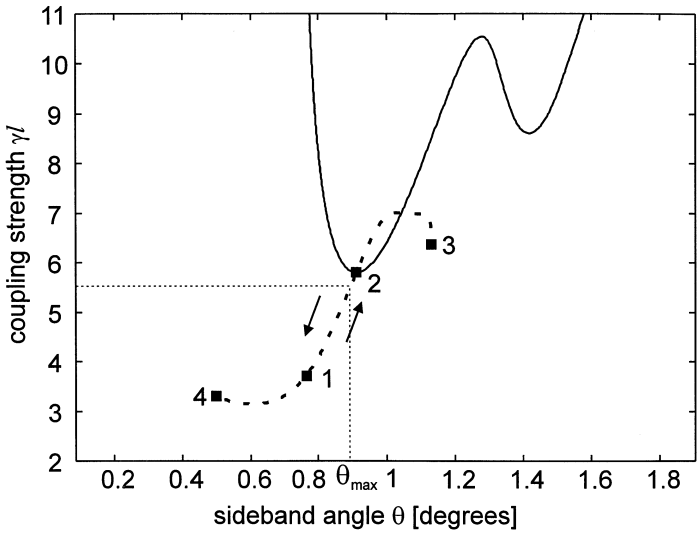

Fig. 3. Threshold curve for normalized propagation length $n_0L/l = -0.7$ (solid line) and curve of the minima for all parameter values $-1 \leqslant n_0L/l \leqslant 1$ (dashed). Selected parameter values are $n_0L/l = -1$ and 0 (point 1), $n_0L/l = -0.7$ and -0.3 (2), $n_0L/l = -0.5$ (3) and $n_0L/l = 1$ (4).

where $F_{\pm 1}$ and $B_{\pm 1}$ are the relative amplitudes of the spatial sidebands. Assuming a feedback reflectivity of unity and no absorption in the medium (see [7] for details), the threshold condition for transverse instability can be obtained. In Fig. 3, an exemplary plot of the threshold coupling strength γl is shown (solid line) for the normalized propagation length $n_0L/l = -0.7$ (virtual mirror inside the crystal with length l). The graph of the minima of the threshold curves for $-1 \leqslant n_0L/l \leqslant 1$ is displayed in the same figure as a dashed line. This parameter curve starts for $n_0L/l = -1$ (point 1) and increases via point 2 ($n_0L/l = -0.7$). The turning point is denoted as 3 with a parameter value of $n_0L/l = -0.5$. Then, the direction is reversed passing point 2 at $n_0L/l = -0.3$, point 1 at $n_0L/l = 0$ and ending at point 4 at $n_0L/l = 1$. The corresponding angles of sideband generation as a function of the normalized propagation length are shown in Fig. 4. The angle of the sidebands increases with larger L, transits over a sharp rectangular-like plateau and decreases again, showing a symmetry around the central region of the crystal.

3. EXPERIMENTAL PATTERN OBSERVATION

Figure 5 shows the experimental setup in detail. We used a frequency-doubled Nd:YAG Laser operating at a wavelength of 532 nm with a maximum output power of 100 mW. The nominally undoped $KNbO_3$-crystal measured $l = 5.6$ mm along the c-axis and was slightly tilted in order to reduce the influence of reflections from its surfaces. The direction of the crystal's c-axis was chosen to be in the direction of the pump beam, which leads to depletion of the input and amplification of the feedback beam. The beam diameter inside the crystal was approximately 350 μm, the power incident on the crystal was 22 mW and the polarization was chosen to be in the direction of the crystal's a-axis in order to take advantage of the large r_{13}-component of the electrooptic tensor.

Lens 1, with a focal length of $f = 100$ mm, was used to focus the beam into the crystal with the beam waist at its back surface. The $2f$–$2f$-feedback system provides the feedback beam with a controllable position of the feedback mirror, i.e., a change in the transverse scale is possible.

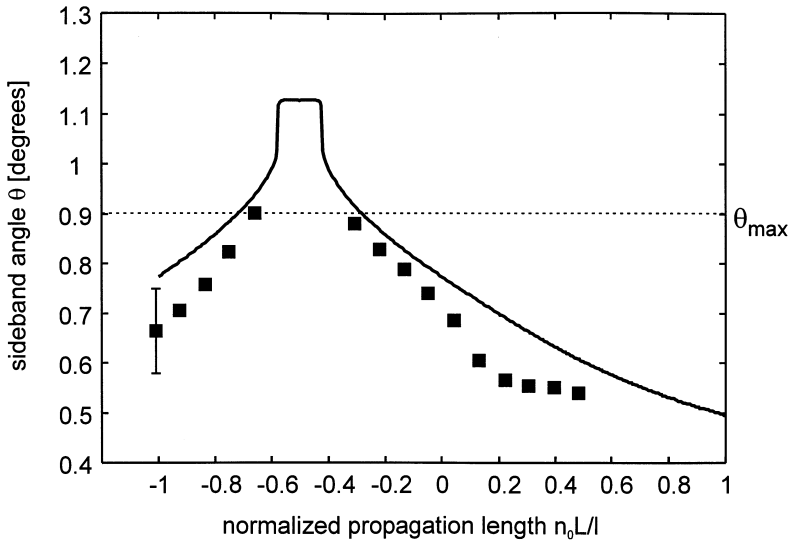

Fig. 4. Sideband angles θ of the far field structure as function of the normalized propagation length n_0L/l, solid line: theory, squares: experiment.

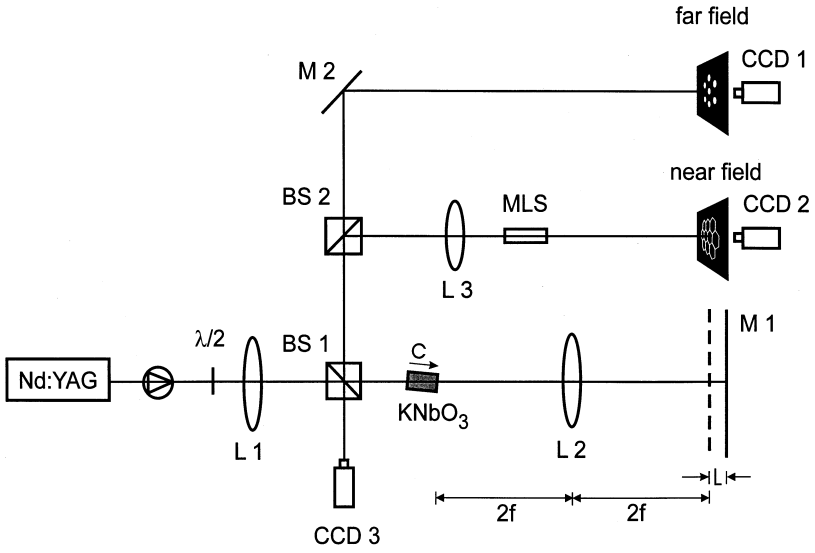

Fig. 5. Experimental setup—L = lens, M = mirror, BS = beamsplitter, MLS = microscope lens system.

Beam splitter 1 enables us to monitor the patterns in the near and far field, and the beam diameter, simultaneously.

The squares in Fig. 4 indicate the experimental results for exactly counterpropagating beams, showing a good agreement with the theoretical treatment. Near the center of the crystal, no patterns could be observed in our recent experiments. This is, in fact, the region where Honda *et al.* observed squares and squeezed hexagons [8]. Maybe the photorefractive coupling constant γ was too small in the present case, as the dashed curve in Fig. 3 indicates. With $\gamma l \approx 6$, a parameter region of $-0.7 \leqslant n_0L/l \leqslant -0.3$ exists, for which the threshold for sideband generation is above

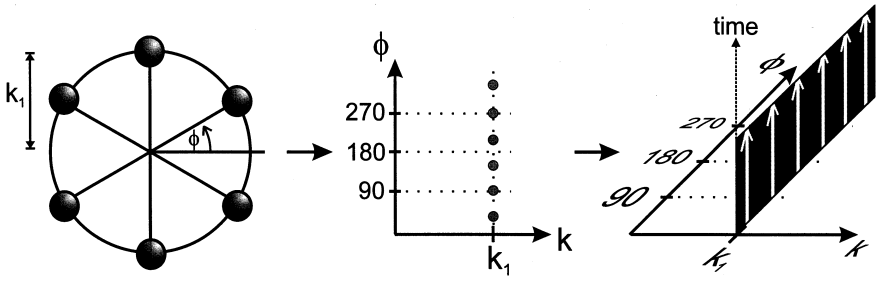

Fig. 6. Visualization method of Thüring *et al.* [10].

the value of γl in the present system. Thus, sidebands with angles $>\theta_{\max}$ cannot be generated. With $\theta_{\max}=0.9^\circ$ (see Fig. 3), the estimated photorefractive coupling strength for the present study is $\gamma l=5.5$. A change of the photorefractive coupling constant, γ, by changing the input beam polarization and a change of the intensity of the incident beam did not result in a measurable change of the transverse scale.

Asymmetries were induced by shifting lens 1 in the transverse direction. As a result of these asymmetries, the photorefractive index grating is read out with a different angle, causing a flow in the near field [9]. Thus, various different spatio-temporal structures can be observed in the far field. At the same time, the asymmetry is a parameter to control the collinearity of the pump and feedback beams, i.e., static hexagonal structures can be achieved in any parameter region by this method. If the reflectivity of the feedback system was reduced, a remarkable transition could be observed: In the region of a feedback reflectivity of $0.25<r<0.35$, roll patterns were favoured, making it possible to observe competition between roll and hexagonal patterns when a small misalignment of the pump with respect to the feedback beam was present. Exactly collinear beams lead to an hexagonal pattern with emphasis on two spots.

4. PATTERN DYNAMICS INDUCED BY NONCOLLINEAR PUMP BEAMS

We are interested in the visualization of the dynamics in this system when a small non-collinearity is introduced and use the method proposed in [10]. Figure 6 gives a quick survey on this effective visualization method. The distribution of spots on a circle with radius k_1 is projected to a linear dimension with the polar coordinate ϕ as the cartesian axis. The time axis is chosen to be perpendicular to this direction and enables us to visualize the dynamics of the system. As a result, every movement of the spots on the circle results in an appropriate pattern change in the cartesian coordinates. For example, a static hexagon causes six stripes, travelling parallel in the positive y-direction (time-axis). The major advantage of this method is that a single image provides us with all the information on the dynamics instead of a sequence of many single pattern images.

Various types of pattern motion have been observed for a maximum feedback reflectivity of $r=0.95$. The favoured situation is the one depicted in Fig. 7. Two stable spots (rolls) and a rocking motion [11] of the other four can be observed, causing us to name it 'Rock n' Roll motion'. The axis determined by the stable spots is always perpendicular to the lens shift and, as a consequence, to the periodic flow in the near field. The frequency of the motion depends linearly on the magnitude of the introduced beam misalignment. Even the orientation of rotation can be reversed by changing the direction of misalignment. In the special case of larger misalignments ($>0.3^\circ$), the movement of the other spots seems to vanish and a roll pattern is left in the far field. Another type of motion is the one depicted in Fig. 8. Here, a slow rotation and a fast leap back

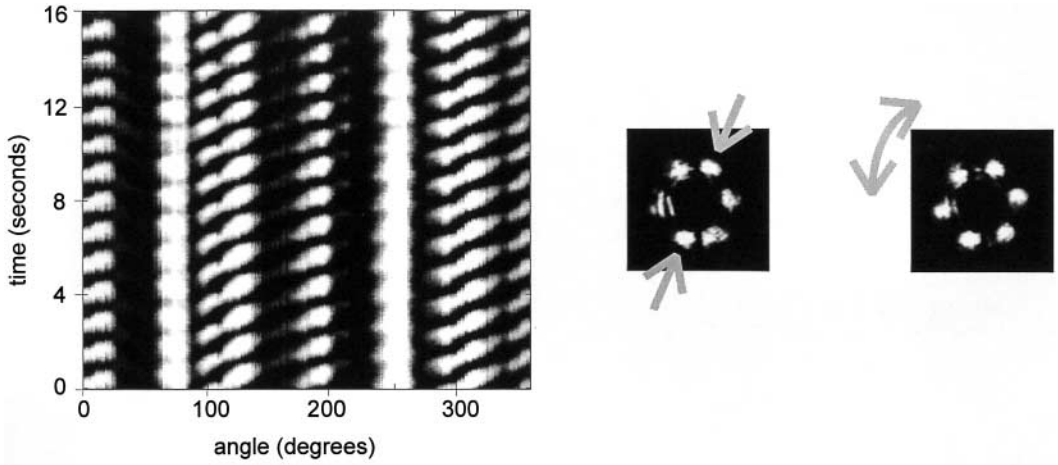

Fig. 7. Rock n' Roll motion with two stable spots (opposite to one another) and a periodic rocking motion of the other four. Left: Temporal evolution, middle and right: motion snapshots indicating the stable spots for this motion.

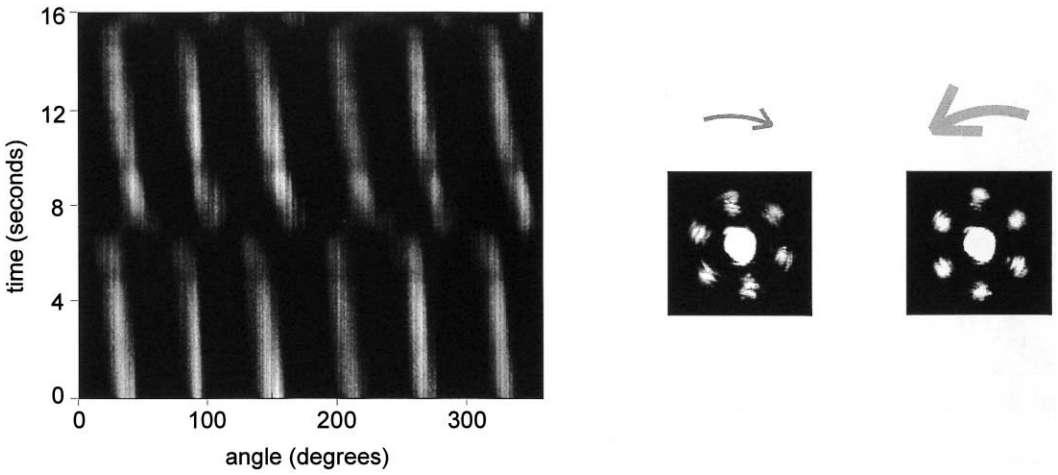

Fig. 8. Rocking motion with all six spots rotating and jumping back to their initial position. Left: Temporal evolution, middle and right: motion snapshots indicating slow rotation and fast leap back.

to the initial position characterizes this movement, which is called rocking motion [11]. Even this motion is temporally stable, but control of the frequency is not as easy as in the case of the Rock n' Roll motion. A small change in the misalignment causes more complex rocking motions, as indicated in Fig. 9. The scenario given here consists of a rocking motion with two different time scales. The regular rocking motion is evident, but even the single spots wobble in a periodic manner with a higher frequency than the one of the rocking motion. The exact parameter regions, e.g., the corresponding angles of misalignment for these different types of motion are currently under investigation.

5. CONCLUSIONS

We have shown that the dynamics of hexagonal pattern formation in a photorefractive feedback system can be induced and controlled by the noncollinearity of the pump-and feedback beams,

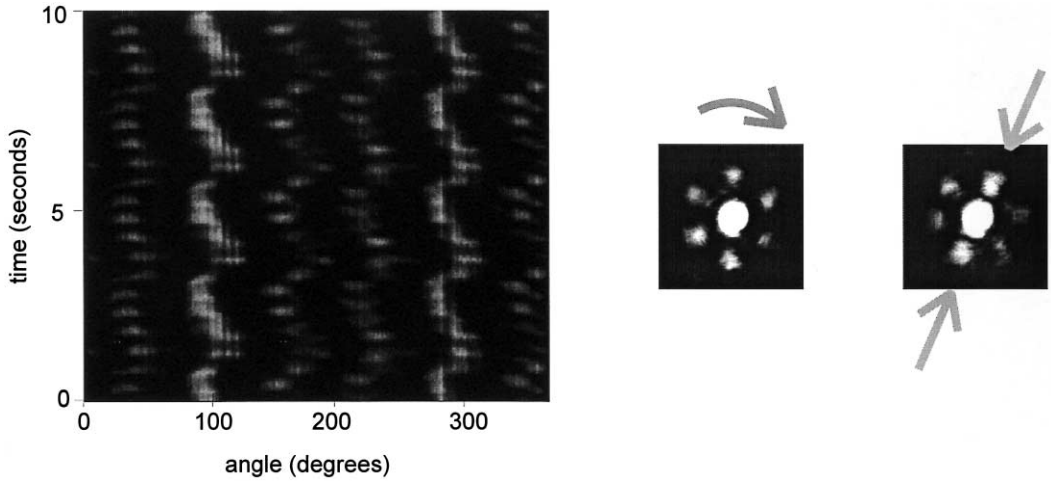

Fig. 9. Complex rocking motion containing two different time scales. Left: Temporal evolution, middle and right: motion snapshots with indicated movement and preferred spots, the other four spots wobble periodically.

whereas the transverse scale depends only on the propagation length. A variety of different scenarios can occur, e.g., situations with stable and moving spots named 'Rock n' Roll motion' and more complicated rotation-like motions. Further investigations concerning the parameter regions for these different types of motion are currently in progress.

Acknowledgements—The authors acknowledge Dr. T. Honda for helpful discussions and for providing the $KNbO_3$-crystal. The experimental work was partially supported by the Deutsche Forschungsgemeinschaft, Sonderforschungsbereich 185, 'Nichtlineare Dynamik'.

REFERENCES

1. Petrossian, A., Pinard, M., Maître, A., Courtois, J. Y., Grynberg, G., Transverse pattern formation for counterpropagating beams in rubidium vapor. *Europhys. Lett.*, 1992, **18,** 689.
2. Tamburrini, M., Bonavita, M., Wabnitz, S., Santamato, E., Hexagonally patterned filamentation in a thin liquid-crystal film with single feedback mirror. *Optics Letters*, 1993, **18,** 855.
3. Thüring, B., Neubecker, R., Tschudi, T., Transverse pattern formation in LCLV feedback system. *Optics Commun*, 1993, **102,** 111.
4. Glückstad, J., Saffman, M., Spontaneous pattern formation in a thin film of bacteriorhodopsin with mixed absorptive dispersive nonlinearity. *Optics Letters*, 1995, **20,** 551.
5. Honda, T., Hexagonal pattern formation due to counterpropagation in $KNbO_3$. *Optics Letters*, 1993, **18,** 598.
6. Honda, T., Matsumoto, H., Buildup of spontaneous hexagonal patterns in photorefractive $BaTiO_3$ with a feedback mirror. *Optics Letters*, 1995, **20,** 1755.
7. Honda, T., Banerjee, P., Threshold for spontaneous pattern formation in reflection-grating-dominated photorefractive media with mirror feedback. *Optics Letters*, 1996, **21,** 779.
8. Honda, T., Matsumoto, H., Sedlatschek, M., Denz, C., Tschudi, T., Spontaneous formation of hexagons, squares and squeezed hexagons in a photorefractive phase conjugator with virtually internal feedback mirror. *Optics Commun.*, 1997, **133,** 293.
9. Honda, T., Flow and controlled rotation of spontaneous optical hexagon in $KNbO_3$. *Optics Letters*, 1995, **20,** 851.
10. Thüring, B., Schreiber, A., Kreuzer, M., Tschudi, T., Spatio-temporal dynamics due to competing spatial instabilities in a coupled LCLV feedback system. *Physica D*, 1996, **96,** 282.
11. Mamaev, A. V., Saffman, M., Modulational instability and pattern formation in the field of noncollinear pump beams. *Optics Letters*, 1997, **22,** 283.